The Journal of Foot & Ankle Surgery 55 (2016) 720–726

Contents lists available at ScienceDirect

The Journal of Foot & Ankle Surgery

journal homepage: www.jfas.org

Diagnostic Value of Elastography in the Diagnosis of Intermetatarsal Neuroma

Tugrul Ormeci, MD [1], Olcay Güler, MD [2], Melih Malkoc, MD [2], Mert Keskinbora, MD [2], Fatma Zeynep Güngören, MD [3], Mahir Mahirogulları, MD [4]

[1] Assistant Professor, Department of Radiology, Medipol University, Faculty of Medicine, Istanbul, Turkey
[2] Assistant Professor, Department of Orthopaedics and Traumatology, Medipol University, Faculty of Medicine, Istanbul, Turkey
[3] Resident, Department of Radiology, Medipol University, Faculty of Medicine, Istanbul, Turkey
[4] Professor and Chairman, Department of Orthopaedics and Traumatology, Medipol University, Faculty of Medicine, Istanbul, Turkey

ARTICLE INFO

Level of Clinical Evidence: 4

Keywords:
elasticity
intermetatarsal space
Morton's neuroma
strain ratio
ultrasound

ABSTRACT

The objective of the present study was to characterize the ultrasound and elastographic properties of intermetatarsal neuroma (interdigital neuroma) and their contribution to diagnosis. Eighteen patients with metatarsalgia, who had presented to an orthopedic clinic from April 2013 to February 2015, were diagnosed with 25 intermetatarsal neuromas (11 unilateral [61.11%], 7 bilateral [38.89%]). These patients underwent evaluation with ultrasonography and simultaneous ultrasound strain elastography to assess the elastographic properties of the tissues in the intermetatarsal space. The intermetatarsal neuroma diagnosis was confirmed by histopathologic inspection. The lesion contours, localization, dimensions, and vascularization were evaluated before surgical excision. The elasticity and strain ratio values were compared between the neuroma and adjacent healthy intermetatarsal space. Of the 25 intermetatarsal neuromas, 1 (4%) was not detected by ultrasonography (incidence of detection of 96%). The mean neuroma width was 6.35 (range 3.7 to 13) mm in the coronal plane, and the mean elasticity and strain ratio values were 3.44 (range 1.1 to 5.1) and 9.47 (range 2.3 to 19.3), respectively. The elasticity and strain ratio values were significantly greater in the presence of an interdigital neuroma than in the adjacent healthy intermetatarsal spaces ($Z = -3.964$, $p = .0001$ and $Z = -3.927$, $p = .0001$, respectively). The diagnostic cutoff values were calculated as 2.52 for elasticity and 6.1 for the strain ratio. Four neuromas (16%) were not demarcated, and the elasticity and strain ratio values for these were lower than those for neuromas with demarcated contours but were greater than those for healthy intermetatarsal spaces ($p < .006$ and $p < .005$, respectively). Patients with clinically suspected intermetatarsal neuromas that do not show demarcation and with smaller lesions might benefit from the use of ultrasound elastography for diagnosis.

Intermetatarsal (Morton's) neuroma is a mechanically triggered entrapment neuropathy of interdigital nerves. Although its exact pathophysiology is still unknown (1,2), it is commonly seen in middle-age females and diagnosed mainly in the third, followed by the second, intermetatarsal space (1–6).

Intermetatarsal neuroma can be diagnosed by careful clinical examination and patient history review (3,7,8). Patients will frequently have a habit of wearing shoes with narrow toe boxes and high heels (1,2,9). Clinical symptoms can vary from pain, numbness, and tingling to burning sensations. In the published data, the tests used for the clinical diagnosis of intermetatarsal neuroma, such as web-space tenderness, foot squeeze, plantar percussion, and toe-tip sensation, have high sensitivities (5,8). The basic principle of those tests is to compress the lesion between the metatarsals, causing pain and sensitivity. Imaging studies have also played an important role (10,11). Imaging studies aid in confirming the diagnosis and detecting asymptomatic and multiple neuromas, as well as possible coexisting pathologies. Ultrasonography (US) is also important in neuroma management (e.g., ultrasound-guided injections). Multiple neuromas will be present in 65% of cases, according to a previous study (5).

Magnetic resonance imaging (MRI) and US are the imaging methods most commonly used in the diagnosis. US has been widely demonstrated as sensitive in detecting interdigital neuroma; however, sometimes, its diagnostic sensitivity has been low, especially for smaller and poorly demarcated lesions (3,12). Moreover, they can be

Financial Disclosure: None reported.
Conflict of Interest: None reported.
Address correspondence to: Tugrul Ormeci, MD, Department of Radiology, Medipol University Faculty of Medicine, Medipol Mega Hastaneler Kompleksi, TEM Avrupa Otoyolu Göztepe çıkışı No: 1 Bağcılar İstanbul 34214, Turkey.
E-mail address: tug_ormeci@yahoo.co.uk (T. Ormeci).

1067-2516/$ - see front matter © 2016 by the American College of Foot and Ankle Surgeons. All rights reserved.
http://dx.doi.org/10.1053/j.jfas.2016.01.025

misdiagnosed as other lesions with similar ultrasound properties. In the study by Saragas (13), the accuracy rate was 97.67%, with 1 lesion misdiagnosed as a ganglion. In such cases, additional methods to increase the sensitivity of US might be necessary.

Elastography is a relatively new technique developed in the 1990s that quantifies the stiffness of a lesion, which has otherwise been evaluated subjectively by physical examination (14). It has since been used to assess various types of tissues, including prostate, breast, liver, thyroid, and musculoskeletal structures (15). Many forms of US elastography are available (e.g., shear-wave and strain). One of the most commonly used forms is strain elastography, also known as compression elastography, real-time elastography, and sonoelastography (16,17). The main principle is that soft tissues will be recompressed or displaced more with application of pressure than will be hard tissues. Patient factors (e.g., size and density in breast tissue), lesion factors (e.g., size, localization, and depth), the properties and capabilities of the US machine, the tissue compression amount and technician-related factors can all have an effect on the elastographic images (18,19). This method involves a comparison of echoes from a particular tissue before and after displacement (14). The lesion elasticity and the elasticity of the surrounding normal tissues are compared (20). Depending on the machine used, different color codes are superimposed over the 2-dimensional images. Stiff areas are marked with blue and soft or elastic tissues with red or green (20). Sonoelastography can provide information on the mechanical properties of the tissues, such as the elasticity and strain ratio, in addition to color mapping of the tissue. Elasticity is the tendency to preserve the tissue's original shape and dimensions. The strain ratio is the degree of the size and shape change occurring with external compression (21). Thus, the strain ratio is a postacquisition assessment that compares lesion deformability with the reference values of the surrounding uninvolved tissue's response to external compression (22).

Elastography has become increasingly common in the evaluation of musculoskeletal systems to determine the presence of Achilles tendinopathy (16), rotator cuff tendinopathy (23), lateral epicondylitis (17), various traumatic and degenerative diseases of the muscles and tendons (24), inflammatory myositis (25), and patellar tendinopathy (26). However, we are aware of only 1 report of elastography for the diagnosis interdigital neuroma. Mossa et al (27) reported that elastography can be used in the diagnosis of intermetatarsal neuroma, but they did not discuss the method in detail. In the present study, we tried to characterize the US and elastographic properties of interdigital neuroma and their contribution to its diagnosis.

Patients and Methods

Study Group Formation

The university ethics board provided ethical approval for the present study. Consecutive patients who had presented to the orthopedics and traumatology departments from April 2013 to February 2015 with pain in the metatarsal region were eligible for inclusion in the present study. Patients with a history of surgery, trauma, or fractures, osteomyelitis seen on radiographs, lesions that might cause foot pain, such as calluses or fungal infections, and/or systemic diseases with joint involvement, such as rheumatoid arthritis, were excluded. Patients without any of the exclusion criteria were included in the present study. These patients underwent surgery after clinical examination and radiologic assessment, and the diagnosis was confirmed by the histopathologic results. Patients who met the inclusion criteria were asked for a detailed history of their disease, and the disease period (period between the onset of symptoms and arrival at the clinic with a complaint) was recorded for each patient. Initially, treatment was planned from the assessment of the patient's history, physical examination results, and radiographic findings. Patients with an unclear diagnosis were referred for advanced imaging studies (US and contrast MRI) to determine a definite diagnosis. The patients with a diagnosis of interdigital neuroma during US examination also underwent simultaneous elastographic evaluations by a radiologist experienced in the musculoskeletal system. The same radiologist also reviewed the MRI scans of the patients in a blinded fashion. Of those patients with a diagnosis of neuroma, those who agreed underwent surgery to allow for histopathologic confirmation.

Radiologic Evaluation

The initial radiologic evaluation included US and strain elastography, followed by MRI to confirm the diagnosis and eliminate other causes of metatarsalgia. All cases were evaluated by a radiologist with 10 years of experience in the musculoskeletal system. US and elastography used a LOGIQ E9 (GE Healthcare GmbH, Munich, Germany) with a linear 9-MHz probe. The examination was performed in the superficial musculoskeletal examination mode, with the appropriate magnification factors. The patients underwent both US and MRI on the same day. US examinations of the foot from the plantar side to the level of the metatarsal head, in the axial and sagittal planes, were performed with the patients in the prone position. In 3 cases with lesions <5 mm, manual pressure was applied only during US imaging (not during elastography) from the dorsal side into the intermetatarsal space to make the lesion more noticeable. Generally, ovoid, hypoechoic (relative to adjacent muscle tissue), noncystic masses with regular contours, oriented parallel to the long axis of the metatarsals at the level of the metatarsal head, were diagnosed as interdigital neuroma (28) (Fig. 1).

The lesion contours, localization, dimensions, and vascularization were evaluated on the US images. Transverse dimensions were measured on the coronal plane image with optimal view of the lesion. The depth could not be measured because of prominent acoustic shadowing caused by the metatarsals.

The standard US analysis was followed by strain elastography, in which the lesion was located on a gray-scale image. The stiffness of a corresponding region of interest (ROI) was assessed on a color map image. In elastography, hard tissues are pseudocolored blue, soft tissues red, and semi-hard tissues green-blue. The stiffness of relatively homogenous fatty tissue without significant plantar fat pad pathology on the same image was used as a reference point. Two ROIs of similar size to the reference ROI were placed on the involved intermetatarsal space, avoiding the metatarsal bones. The reference ROI placed on the fatty tissues could not be placed at the same level as the neuroma because of shadowing from the metatarsal bones. After confirming adequate pressure and that the color scale was homogenous, the elasticity and strain ratio values were measured twice in the lesion and a healthy intermetatarsal space for comparison. For each intermetatarsal space, the elasticity and strain ratio values were calculated by taking the mean of 2 measurements. The intermetatarsal bursal fluid, presence of bursitis, and nonspecific edema or inflammation of the soft tissue on the plantar side of the foot, which can accompany interdigital neuromas, were also evaluated.

Surgical Procedure

Of the 45 patients diagnosed with interdigital neuroma after a review of the patient's history and clinical examination, MRI, US, and elastographic evaluation results, 18 patients (25 interdigital neuromas; 40% of 45 patients) agreed to surgery and underwent dissection of the intermetatarsal space and excision of a plantar intermetatarsal neuroma. All the patients were treated with oral anti-inflammatory drugs, injection of local anesthetic and corticosteroids in the symptomatic intermetatarsal space, physical therapy, foot orthoses and insole modification, alteration of weight-bearing activities, and immobilization. Only those patients without a satisfactory response after $\geq$12 weeks of nonsurgical therapy subsequently underwent neuroma excision. Those patients with failure of nonoperative therapy underwent surgery from a dorsal approach, with the patients under general anesthesia and using limb exsanguination and a pneumatic tourniquet. The deep transverse intermetatarsal ligament was cut to free the entrapped, plantar common digital nerve. Operatively, a neuroma was identified by the presence of perineural and intraneural fibrosis and enlargement of the entrapped nerve trunk. The abnormal nerve was excised proximal to the proximal margin of the deep transverse intermetatarsal ligament, and the transected proximal nerve stump was allowed to retract proximally into the intact intrinsic

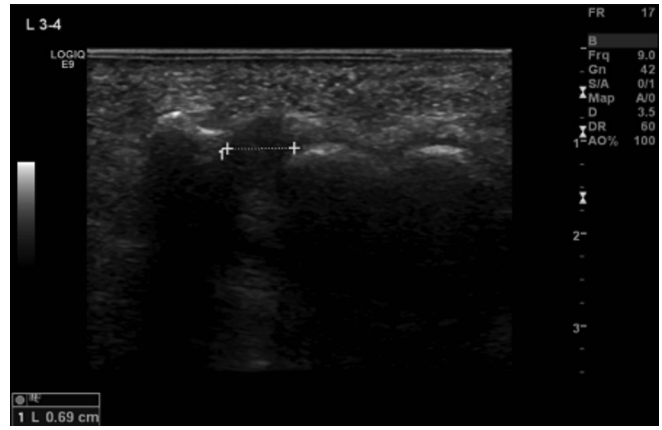

Fig. 1. Coronal ultrasound image showing a well-circumscribed, ovoid, and hypoechoic (relative to adjacent muscle) mass in the third intermetatarsal space of the left foot, consistent with Morton's neuroma.

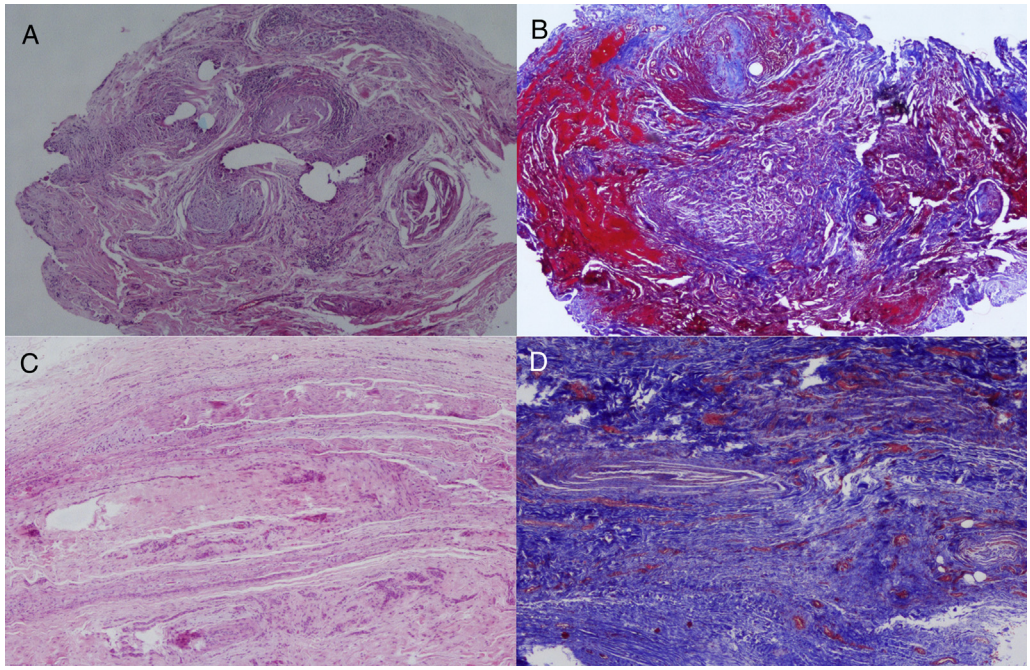

Fig. 2. Histologic views of 2 different interdigital neuroma cases. (*A* and *B*) Images showing an earlier stage lesion than the stage in the second case (*C* and *D*). (*A* and *C*) The nerves show stromal edema and mild myxoid changes (hematoxylin-eosin stain, original magnification ×40). (*D*) Epineural thickening surrounding the nerve is more prominent than in Fig. B. (*D*) Marked fibrosis showing a *darker blue* stain with Masson's trichrome stain (*B* and *D*, Masson's trichrome stain, original magnification ×40).

skeletal muscle bellies. The excised nerve lesion was embedded in formalin and submitted for pathologic examination. In each case, the histopathologic results confirmed the diagnosis of neuroma (Fig. 2).

Statistical Analysis

The data were characterized using descriptive statistical methods (i.e., frequency, percentage, mean, standard deviation, and minimum and maximum). Spearman's rho and Pearson's correlation coefficient and partial correlation were used to define the relationships, and the chi-square, *t*, and Mann-Whitney *U* tests were used to define the differences. Receiver operating characteristic (ROC) curve analysis was performed for test differentiation. All results were assessed at the 95% confidence interval and 5% ($p \leq .05$) significance level. SPSS, version 15.0 (SPSS Inc., Chicago, IL), and Microsoft Excel 2007 (Microsoft, Redmond, WA) were used for the analyses.

Results

The data from 447 consecutive patients with pain in the forefoot who had visited the orthopedics clinic from April 2013 to February 2015 were reviewed. In their initial examination, 344 patients (76.96%) were diagnosed from the patient history, physical examination findings, and direct radiographic imaging results, and treatment was planned accordingly. The remaining 103 patients (23.04%) underwent additional imaging studies with US and contrast MRI examinations. An interdigital neuroma was detected in 45 patients (10.07%) using US examination by a radiologist with 10 years of experience with the musculoskeletal system. These 45 patients underwent simultaneous elastographic evaluation. The MRI results of the 103 patients (23.04%) were assessed by the same radiologist without knowledge of the patients' diagnosis.

In the 45 patients (10.07%) with an intermetatarsal neuroma, a strong correlation was found between the MRI and US-elastographic findings of the presence of a neuroma. Of these 52 neuromas in 45 patients, 28 (53.9%) were localized to the third intermetatarsal space, 23 (44.2%) to the second intermetatarsal space, and 1 (1.9%) to the first intermetatarsal space. One neuroma (1.9%) was observed on MRI but was not detected using US. The 45 patients were informed of their treatment options, and 18 (40%; 25 interdigital neuromas) agreed to undergo surgery. The histopathologic results confirmed the neuroma diagnosis for all 18 patients. These 25 interdigital neuroma cases from 18 patients (12 females [66.7%] and 6 males [33.3%]) were included in the present study. The mean patient age was 40.33 (range 21 to 65) years, the mean disease duration of metatarsalgia was 27.04 (range 1 to 120) months, and the mean neuroma size (width) was 6.35 (range 3.7 to 13) mm in the coronal plane. The neuromas in the second intermetatarsal space had a mean size of 5.63 (range 5 to 6.3) mm, and

Table
Relationship between elasticity and strain ratio of intermetatarsal spaces stratified by localization (N = 24 neuromas in 18 patients)

Variable	Average	*p* Value*	Intermetatarsal Space		
			First	Second	Third
Intermetatarsal neuroma (N)	24		1 (4.2)	5 (20.8)	18 (75)
Size† (mm)		.59‡			
Mean	6.35		9.5	5.63	6.34
Range	3.7 to 13			5 to 6.3	3.7 to 13
Elasticity		.0001			
Normal					
Mean	1.55		2.55	2.05	1.38
Range	0.7 to 2.55				0.7 to 2.5
Neuroma					
Mean	3.44		3.9	3.24	3.48
Range	1.1 to 5.1			2.1 to 4.3	1.1 to 5.1
Strain ratio		.0001			
Normal					
Mean	3.86		6.2	5.15	3.46
Range	1.45 to 6.2				1.45 to 6
Neuroma					
Mean	9.47		13.6	8.52	9.5
Range	2.3 to 19.3			5.5 to 11.25	2.3 to 19.3

Data in parentheses are percentages.
* Mann-Whitney *U* test.
† Width in coronal plane.
‡ Statistically significant difference between second and third intermetatarsal spaces (Mann-Whitney *U* test).

those in the third intermetatarsal space averaged 6.34 (range 3.7 to 13) mm (Table). All neuromas appeared hypoechoic, without prominent blood flow; the interdigital nerve was not detectable. Intermetatarsal bursitis, which can be associated with neuroma, was not detected on US.

Patient age, disease duration, and interdigital neuroma size measured by US did not correlate with the elasticity or strain ratio measurements ($p > .05$). Disease duration and patient age had no statistically significant relationship ($r = 0.0001$; $p = .998$). The size of the neuromas located in the second and third intermetatarsal spaces did not differ significantly ($p > .05$).

Of the 25 interdigital neuromas, 1 could not be diagnosed by US (incidence of detection 96%). Specificity was not calculated, because histopathologic confirmation of a neuroma in a patient with normal US results could not be obtained for every case. The remaining neuromas were found in the first intermetatarsal space in 1 (4.2%), the second intermetatarsal space in 5 (20.8%), and the third intermetatarsal space in 18 (75%) cases (Table); 7 patients (38.9%) were diagnosed with multiple neuromas.

All 24 neuromas were hypoechoic, 20 had sharp borders, and 4 did not have a clear demarcation. The elasticity and strain ratio values of the neuromas without a clear demarcation were greater than those of the healthy intermetatarsal spaces ($p < .006$ and $p < .005$, respectively). The mean elasticity of the neuromas was 3.44 (range 1.1 to 5.1), and the mean strain ratio was 9.47 (range 2.3 to 19.3). These values were greater than those of the normal intermetatarsal spaces without apparent interdigital neuroma lesions: 1.55 (range 0.7 to 2.55) and 3.86 (range 1.45 to 6.2), respectively (Table). The elasticity and strain ratio values of the neuromas in the second intermetatarsal space were 3.24 (range 2.1 to 4.3) and 8.52 (range 5.5 to 11.25), respectively, and those of neuromas in the third intermetatarsal space were 3.48 (range 1.1 to 5.1) and 9.5 (range 2.3 to 19.3), respectively (Table). The mean elasticity and strain ratio values of the interdigital neuromas were significantly greater than the elasticity and strain ratio values of the nonpathologic intermetatarsal spaces ($Z = -3.964$, $p = .0001$ and $Z = -3.927$, $p = .0001$, respectively).

The percentage of change in the elasticity values between the normal and pathologic intermetatarsal spaces was calculated. The elasticity values of the neuromas were 220% greater than those of normal intermetatarsal spaces, with an increase in the strain ratio values of 245%. In 24 interdigital neuromas, the elasticity and strain ratio values both had significant effects on the differential diagnosis ($p = .0001$). The area under the ROC curve was 0.92 (range 0.85 to 0.99; $p = .0001$), and the cutoff elasticity value was 2.52 (sensitivity 0.75 and specificity 0.91). The area under the ROC curve was 0.92 (0.83 to 0.99; $p = .0001$), and the cutoff strain ratio value was 6.1 (sensitivity 0.75 and specificity 0.91).

Discussion

Although interdigital neuroma is diagnosed mainly from the patient history and clinical examination findings, imaging studies are also used for the differential diagnosis, exact localization of the lesion, and the detection of additional neuromas and for legal reasons (11,29). US has been the most common imaging method used because of its ease of access and use, cost-effectiveness, rapid results, and applicability to all patients. However, smaller lesions that do not significantly cross intermetatarsal lines to the plantar surface can be a challenge to diagnose using US. Additionally, the changes in echogenicity with lesion maturity can make it more difficult to differentiate neuromas from the surrounding fat planes. Thus, US might need to be supplemented with another imaging modality in such cases.

Currently, with advances in technology, elastography is used in many organs in conjunction with US. Elasticity is defined as tissue deformability on application of an external force and resumption of the original shape when the force has been removed. The force of the operator's applied pressure is displayed in real time on the monitor, allowing for the selection of the optimal compression depending on the strain. Strain elastography evaluates elasticity both qualitatively and semiquantitatively (30,31).

US sensitivity has been reported to be 56.5% to 100% in published studies (4,7,29,32–35). Likewise, the mean size of interdigital neuromas has been reported to vary from 4.9 to 7.4 mm (3,4,11,33,35,36). Neuromas >5 mm in size are more likely to cause symptoms (9,28,33,37). In our study, the mean neuroma size on US examination was 6.35 (range 3.7 to 13) mm, and 21 (87.5%) were >5 mm. Our incidence of detection was 96%.

We noticed interdigital neuromas in the third intermetatarsal space most often (18 neuromas; 75%), in agreement with the findings from other studies (1,9,37). Multiple neuromas were reported by Valero et al (38) to be more frequent (65.2% of all cases) than previously thought. In contrast, we observed multiple neuromas in 7 of 18 patients (38.9%). No significant correlation was found between patient age and elastography values or between neuroma size and localization or disease duration.

One of the most important factors affecting the neuroma detection rate by US is whether the lesion crosses the intermetatarsal line toward the plantar surface. Of our 25 cases, 17 (70.83%) had significant plantar extension, and 7 (29.17%) had minimal extension. In the 1 case in which we could not detect the neuroma, we believe it was not identifiable because it was <5 mm and was 1 of multiple neuromas.

Hypoechoic areas caused by lumbrical muscles and flexor digitorum tendons and acoustic shadowing caused by metatarsal heads could prevent obtaining an optimal view of the lesion (Fig. 3) or cause the neuroma to appear larger than its actual size. However, identifying the correct location by US before performing elastography measurements is key to preventing errors but is challenging because of the location of interdigital neuromas within a closed, small area surrounded by the dorsal and plantar interosseous tendons, lumbrical muscles, and metatarsals (Fig. 3). The measurements must be taken at the level of the metatarsal head. Examining patients in an oblique prone position, such as was done in some of our patients, will help to account for variations in metatarsal dimension and shape. This strategy will also help pinpoint neuroma localization using a probe and allows a clearer view of lesions that extend from the intermetatarsal area toward the interphalangeal space, enabling elastography measurements of the lesion area.

Regardless of the intermetatarsal space differences, the mean neuroma elasticity was 3.44 (range 1.1 to 5.1), and the mean strain ratio was 9.47 (range 2.3 to 19.3; Fig. 4). In healthy individuals with no pathologic features in the intermetatarsal area, the mean elasticity of the same location was 1.55 (range 0.7 to 2.55), and the mean strain ratio was 3.86 (range 1.45 to 6.2). The elasticity and strain ratio values were significantly greater for interdigital neuromas than for uninvolved intermetatarsal spaces ($Z = -3.964$, $p = .0001$ and $Z = -3.927$, $p = .0001$, respectively).

Interdigital neuroma histopathologic findings include intraneural and perineural fibrosis, increased arteriolar blood vessels and decreased calibration of blood vessels, edema of the endoneurium, axonal degeneration, infiltration of leukocytes, and epineural and endoneural vascular hyalinization (2,5,6,38) (Fig. 2). Previous studies have reported interdigital nerves within neuromas (39); however, we could not visualize nerves using US. Edema, axonal degeneration, and fibrosis can affect echogenicity and elasticity.

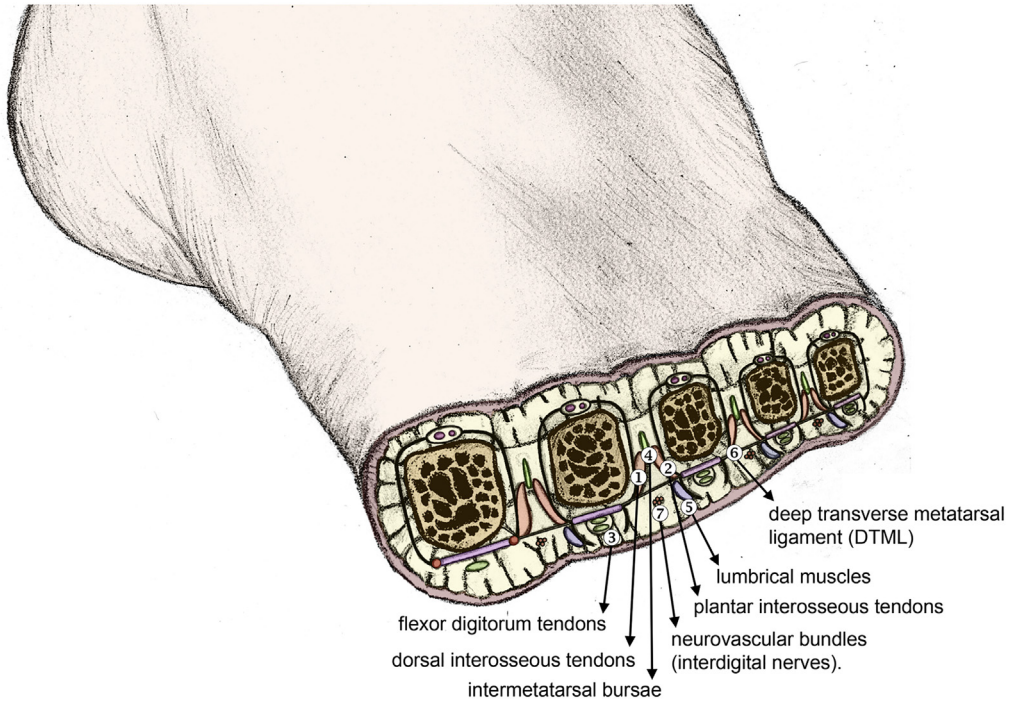

Fig. 3. Coronal view of intermetatarsal spaces at the metatarsal head level: 1, dorsal interosseous tendons; 2, plantar interosseous tendons; 3, flexor digitorum tendons; 4, intermetatarsal bursae; 5, lumbrical muscles; 6, deep transverse metatarsal ligament; and 7, neurovascular bundles (interdigital nerves).

Early in their development, neuroma elasticity will be is heterogeneous (green-blue tones on the color map; Fig. 5). In advanced cases, the blue shades, correlating with greater elasticity and strain ratio values, will be more prominent, probably owing to increased fibrosis (Fig. 6). This finding is in agreement with studies reporting the positive reaction (good recovery) of early neuromas to injections of hydrocortisone and local anesthetic. However, the fibrofatty mass surrounding pathologically degenerated and edematous nerves appears hypoechoic on US, and effusions at the neuroma site owing to inflammatory responses are also common. With time, it will become more difficult to differentiate the neuroma from the surrounding tissues as the lesion solidifies (12). In our clinical experience, sonoelastography is useful in detecting lesions, especially those that are poorly demarcated. In our study, most of the neuromas had hypoechoic areas with clearly defined borders, although 4 neuromas were also hypoechoic and had more blurred borders, similar to those of adjacent intermetatarsal spaces and making differentiation difficult. The latter US appearance was reported by Betts et al (12) to occur in 80% of control patients. Their differentiation strategy involved comparing hypoechoic areas with blurred borders with those of intermetatarsal neuromas (12). These "echo-poor" areas are likely to represent small, asymptomatic changes to the nerve and surrounding soft tissue caused by irritation and could account for some unsuccessful surgical outcomes. We also noted similar hypoechoic and asymptomatic areas within the adjacent intermetatarsal space, even when the US view slightly crossed the intermetatarsal line. The color map values of those areas were sometimes different from those of the normal intermetatarsal spaces. These difficulties can be solved using elastographic evaluation in conjunction with US. The elasticity and strain ratio values of neuromas increased by 220% and 245%, respectively, compared with the uninvolved intermetatarsal spaces. Because the difference in elasticity and strain ratio between interdigital neuroma and normal intermetatarsal spaces was statistically significant, using ROC curves helped determine which hypoechoic areas were, in fact, neuromas. The cutoff values for elasticity and strain

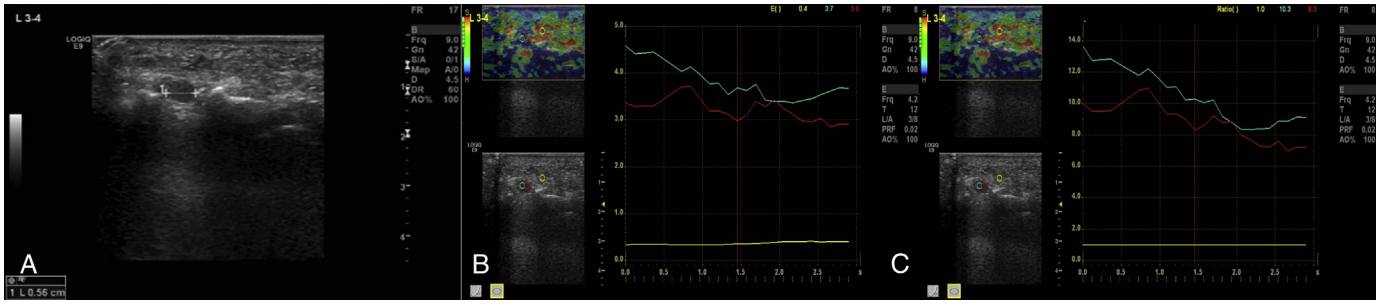

Fig. 4. View of a 45-year-old female with metatarsalgia. (*A*) Coronal ultrasound image showing a well-circumscribed, ovoid, and hypoechoic mass lesion in the third intermetatarsal space of the left foot, consistent with Morton's neuroma. The mean elasticity of the 2 regions of interest was 3.35 (*B*), and the mean strain ratio was 9.3 (*C*). The lesion was slightly heterogeneous but appeared mostly *blue* on the color map.

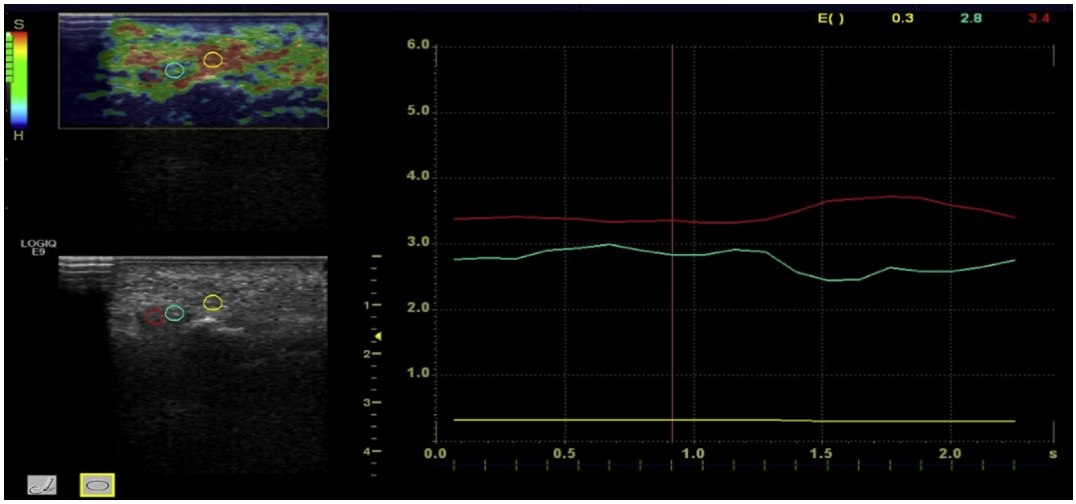

Fig. 5. Coronal ultrasound image of the third intermetatarsal space of the left foot showing a solid hypoechoic lesion, consistent with Morton's neuroma, appearing heterogeneous but mostly *green-blue* on the color map, as seen in early-stage cases.

ratio were 2.52 (sensitivity, 0.75; specificity, 0.91; Fig. 7A) and 6.1 (sensitivity, 0.75; specificity, 0.91; Fig. 7B), respectively.

In those neuromas without clear demarcation, the elasticity and strain ratio values were lower than those for neuromas with demarcated contours; however, the differences were not statistically significant ($p = .814$ and $p = .727$, respectively). The mean duration of disease in those cases was 2.7 months. The elasticity and strain ratio values of the neuromas without clear demarcation were greater than those of the healthy intermetatarsal spaces. We think that the lower elasticity and strain ratio values in those cases resulted from the increased accompanying inflammatory responses during the early stages of the disease, making contour clarification difficult. Thus, in those cases, the neuromas sometimes could not be distinguished from the adjacent fat planes. Again, soft tissue pathologic features seen on the plantar side, such as adventitial bursitis or intermetatarsal bursitis, can present a challenge in the differential diagnosis. In those cases, elastography can provide useful additional information to the US findings. However, no significant relationship was found between the disease duration and the elasticity or strain ratio values ($p > .05$). This was probably because the disease duration was obtained from the patients, whose memory is somewhat questionable in terms of reliability. In the pathologic evaluation of the specimens, the cases with higher elasticity and strain ratio values also had greater amounts of fibrosis in the interdigital neuromas (Fig. 2). In the published data, it has often been reported that inflammation is more common during the early stages of interdigital neuromas and that it solidifies with lesion maturation (12). Thus, we believe that the disagreement between the disease duration and elasticity values resulted mainly from the patients' failure to remember exactly when their symptoms began or from the small sample size.

The greatest limitation of our study was the relatively small number of cases. Although the color map evaluations were clear, the elasticity and strain ratio values might not be homogeneous among patients. Nonhomogeneity mainly results from the inclusion of interdigital nerves, lumbrical muscles, interosseous tendons, and/or surrounding reactive edema or inflammation or fibrosis inside the ROI. In the published data, no elasticity study on interdigital neuroma for comparison. We hope that our findings will lead to additional studies with larger sample sizes.

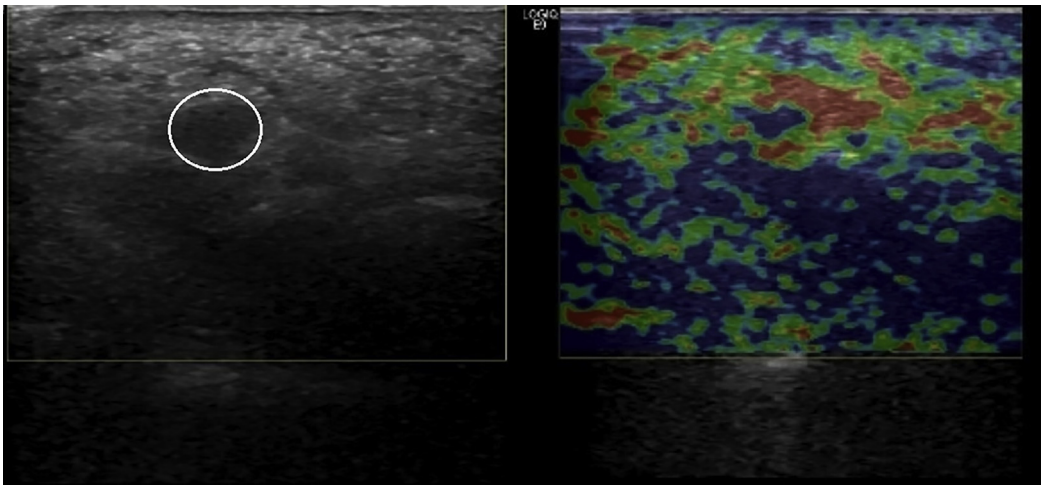

Fig. 6. Coronal ultrasound image showing a solid hypoechoic lesion in the third intermetatarsal space of the left foot, consistent with Morton's neuroma. It appears *blue* on the color map, as seen in long-term cases.

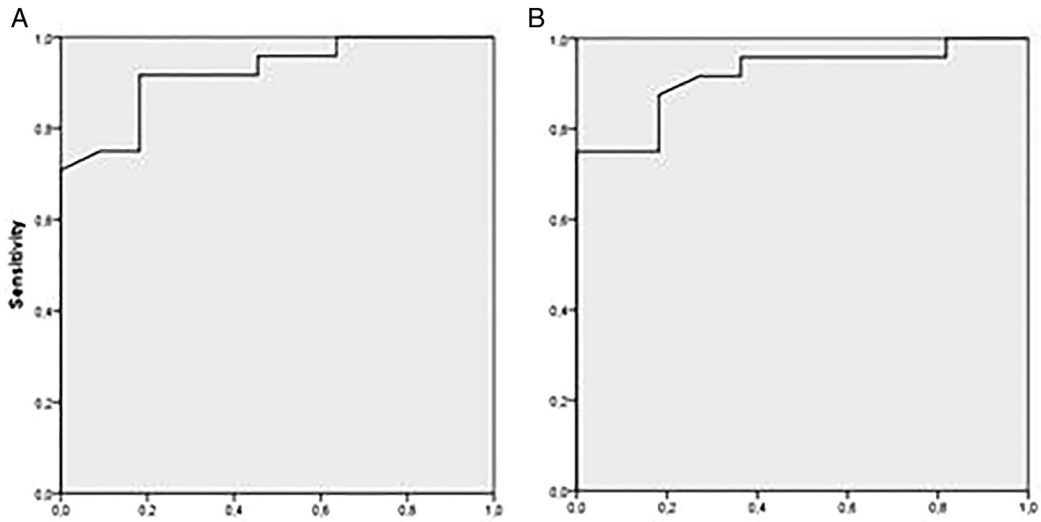

Fig. 7. Graph of receiver operating characteristic curves for elasticity (*A*) and strain ratio (*B*) measured using elastography.

In conclusion, US with elastographic evaluation constitutes a useful modality with high sensitivity for interdigital neuroma diagnosis. Strain elastography is a beneficial and promising imaging method because of its relatively short interpretation period and examination time, low cost, and real-time monitoring of interdigital neuromas. Thus, patients with clinically suspected interdigital neuromas that do not show lesion demarcation, because of their small size, can be diagnosed using of US elastography.

References

1. Lee MJ, Kim S, Huh YM, Song HT, Lee SA, Lee JW, Suh JS. Morton neuroma: evaluated with ultrasonography and MR imaging. Korean J Radiol 8:148–155, 2007.
2. Jain S, Mannan K. The diagnosis and management of Morton's neuroma: a literature review. Foot Ankle Spec 6:307–317, 2013.
3. Williams RL, Grace DL, Papas J. Ultrasonography in the diagnosis of Morton's neuroma. Foot 6:159–162, 1996.
4. Irwin LR, Konstantoulakis C, Hyder NU, Sapherson DA. Ultrasound in the diagnosis of Morton's neuroma. Foot 10:186–189, 2000.
5. Owens R, Gougoulias N, Guthrie H, Sakellariou A. Morton's neuroma: clinical testing and imaging in 76 feet, compared to a control group. Foot Ankle Surg 17:197–200, 2011.
6. Quinn TJ, Jacobson JA, Craig JG, van Holsbeeck MT. Sonography of Morton's neuromas. AJR Am J Roentgenol 174:1723–1728, 2000.
7. Kaminsky S, Griffin L, Milsap J, Page D. Is ultrasonography a reliable way to confirm the diagnosis of Morton's neuroma? Orthopedics 20:37–39, 1997.
8. Pastides P, El-Sallakh S, Charalambides C. Morton's neuroma: a clinical versus radiological diagnosis. Foot Ankle Surg 18:22–24, 2012.
9. Bencardino J, Rosenberg ZS, Beltran J, Liu X, Marty-Delfaut E. Morton's neuroma: is it always symptomatic? AJR Am J Roentgenol 175:649–653, 2000.
10. Zanetti M, Strehle JK, Kundert HP, Zollinger H, Hodler J. Morton neuroma: effect of MR imaging findings on diagnostic thinking and therapeutic decisions. Radiology 213:583–588, 1999.
11. Kankanala G, Jain AS. The operational characteristics of ultrasonography for the diagnosis of plantar intermetatarsal neuroma. J Foot Ankle Surg 46:213–217, 2007.
12. Betts RP, Bygrave CJ, Jones S, Smith TWD, Flowers MJ. Ultrasonic diagnosis of Morton's neuroma: a guide to problems, pointers, pitfalls and prognosis. Foot 13:92–99, 2003.
13. Saragas NP. Hydrocortisone/local anaesthetic injection versus ultrasound in the diagnosis of interdigital neuroma. Foot Ankle Surg 12:149–151, 2006.
14. Barr RG. Sonographic breast elastography. J Ultrasound Med 31:773–783, 2012.
15. Ginat DT, Destounis SV, Barr RG, Castaneda B, Strang JG, Rubens DJ. US elastography of breast and prostate lesions. Radiographics 29:2007–2016, 2009.
16. Drakonaki EE, Allen GM, Wilson DJ. Real-time ultrasound elastography of the normal Achilles tendon: reproducibility and pattern description. Clin Radiol 64:1196–1202, 2009.
17. De Zordo T, Lill SR, Fink C, Feuchtner GM, Jaschke W, Bellmann-Weiler R, Klauser AS. Real-time sonoelastography of lateral epicondylitis: comparison of findings between patients and healthy volunteers. AJR Am J Roentgenol 193:180–185, 2009.
18. Itoh A, Ueno E, Tohno E, Kamma H, Takahashi H, Shiina T, Yamakawa M, Matsumura T. Breast disease: clinical application of US elastography for diagnosis. Radiology 239:341–350, 2006.
19. Thomas A, Fischer T, Frey H, Ohlinger R, Grunwald S, Blohmer JU, Winzer KJ, Weber S, Kristiansen G, Ebert B, Kümmel S. Real-time elastography—an advanced method of ultrasound: first results in 108 patients with breast lesions. Ultrasound Obstet Gynecol 28:335–340, 2006.
20. Burnside ES, Hall TJ, Sommer AM, Hesley GK, Sisney GA, Svensson WE, Fine JP, Jiang J, Hangiandreou NJ. Differentiating benign from malignant solid breast masses with US strain imaging. Radiology 245:401–410, 2007.
21. Wells PN, Liang HD. Medical ultrasound: imaging of soft tissue strain and elasticity. J Royal Soc Interface 54:1–29, 2011.
22. Chiorean A, Duma MM, Dudea SM, Iancu A, Dumitriu D, Roman R, Sfrangeu S. Real-time ultrasound elastography of the breast: state of the art. Med Ultrason 10:73–82, 2008.
23. Silvestri E, Garlaschi G, Bartolini B, Minetti G, Schettini D, D'Auria MC, Cimmino MA. Sonoelastography can help in the localization of soft tissue damage in polymyalgia rheumatica (PMR). Clin Exp Rheumatol 25:796, 2007.
24. Grainger AJ. Highlights of the European Society of Musculoskeletal Radiology (ESSR) annual meeting 2010. Skeletal Radiol 40:137–139, 2011.
25. Botar-Jid C, Damian L, Dudea SM, Vasilescu D, Rednic S, Badea R. The contribution of ultrasonography and sonoelastography in assessment of myositis. Med Ultrason 12:120–126, 2010.
26. Khan KM, Maffulli N, Coleman BD, Cook JL, Taunton JE. Patellar tendinopathy: some aspects of basic science and clinical management. Br J Sports Med 32:346–355, 1998.
27. Mossa PM. Morton's neuroma. MCO Orthop Med Surg 2:21–23, 2014.
28. Redd RA, Peters VJ, Emery SF, Branch HM, Rifkin MD. Morton neuroma: sonographic evaluation. Radiology 171:415–417, 1989.
29. Zanetti M, Ledermann T, Zollinger H, Hodler J. Efficacy of MR imaging in patients suspected of having Morton's neuroma. AJR Am J Roentgenol 168:529–532, 1997.
30. Ueno E, Itoh A. Diagnosis of breast cancer by elasticity imaging. Eizo Joho Med 36:2–6, 2004.
31. Rubaltelli L, Corradin S, Dorigo A, Stabilito M, Tregnaghi A, Borsato S, Stramare R. Differential diagnosis of benign and malignant thyroid nodules at elastosonography. Ultraschall Med 30:175–179, 2009.
32. Torres-Claramunt R, Ginés A, Pidemunt G, Puig L, de Zabala S. MRI and ultrasonography in Morton's neuroma: diagnostic accuracy and correlation. Indian J Orthop 46:321–325, 2012.
33. Pollak RA, Bellacosa RA, Dornbluth NC, Strash WW, Devall JM. Sonographic analysis of Morton's neuroma. J Foot Surg 31:534–537, 1992.
34. Shapiro PP, Shapiro SL. Sonographic evaluation of interdigital neuromas. Foot Ankle Int 16:604–606, 1995.
35. Sobiesk GA, Wertheimer SJ, Schulz R, Dalfovo M. Sonographic evaluation of interdigital neuromas. J Foot Ankle Surg 36:364–366, 1997.
36. Sharp RJ, Wade CM, Hennessy MS, Saxby TS. The role of MRI and ultrasound imaging in Morton's neuroma and the effect of size of lesion on symptoms. J Bone Joint Surg Br 85:999–1005, 2003.
37. Zanetti M, Strehle JK, Zollinger H, Hodler J. Morton neuroma and fluid in the intermetatarsal bursae on MR images of 70 asymptomatic volunteers. Radiology 203:516–520, 1997.
38. Valero J, Gallart J, González D, Deus J, Lahoz M. Multiple interdigital neuromas: a retrospective study of 279 feet with 462 neuromas. J Foot Ankle Surg 54:320–322, 2015.
39. Simmons DN. Imaging of the Painful Forefoot. Techn Foot Ankle Surg 7:238–249, 2008.